

Temperature and pressure dependence of the optical absorption in hexagonal MnTe

Ch. Ferrer-Roca,* A. Segura, C. Reig, and V. Muñoz

Institut de Ciència dels Materials, Departament de Física Aplicada, Universitat de València, Dr. Moliner 50, 46100 Burjassot, Valencia, Spain

(Received 28 December 1999)

The absorption edge of hexagonal (NiAs structure) antiferromagnetic MnTe has been measured by means of light transmission experiments carried out at different temperatures in the range 16–420 K ($P=1$ bar) and hydrostatic pressures up to 9 GPa ($T=295$ K). An indirect band gap has been found, in agreement with previous band-structure calculations, with an energy of $E_{ig}=1.272\pm 0.013$ eV at room temperature and pressure. The temperature dependence of the absorption edge is linear above the Néel temperature $T_N=310$ K, with a temperature coefficient $dE/dT=-(3.5\pm 0.1)\times 10^{-4}$ eV/K. Below T_N an additional blueshift is found, with a maximum value of 0.1 eV at low temperatures. The temperature dependence of this anomalous shift is proportional to the square of the magnetization, a result which is consistent with previous second-order perturbation calculations. Regarding the measurements under pressure, a negative pressure coefficient with a value of $dE/dP=-(59\pm 2)$ meV/GPa has been found. The Néel temperature is known to increase with pressure in hexagonal MnTe, due to an increment of the exchange interaction, or equivalently, of the sublattice magnetization. Consequently a positive pressure shift could be expected at room temperature, derived from both the antiferromagnetic splitting of Mn 3d orbital and second-order electron and hole interaction with fixed Mn spins. The negative pressure coefficient has thus been interpreted as a sum of that positive contribution and a larger negative one derived from an enhanced p - d repulsion which would lead to an upwards shift of the valence-band maximum.

I. INTRODUCTION

Compounds containing 3d transition metals have attracted considerable attention in the past decade due to the large variety of transport and magneto-optical properties they display, owing to the presence of a significant magnetic moment, especially in the case of compounds which include manganese, with a 3d⁵ configuration. Hexagonal (*H*) MnTe is an antiferromagnetic (AF) compound with a stable bulk NiAs structure, although it can also crystallize in a NaCl phase at $T>1040$ °C or in a zinc-blende (ZB) phase if grown by molecular-beam epitaxy.¹ *H*-MnTe is a particularly interesting example of a transition-metal compound as most materials belonging to this group (MnSb, for example) are metallic, whereas other manganese compounds, such as the chalcogenides MnS, MnSe, and MnO, with a stable NaCl crystallographic structure, are insulators. Therefore, MnTe is one of the few semiconductors known in this family, a *crossroads* material, as pointed out by Allen *et al.*² The properties of *H*-MnTe have been the subject of several works in the past, although not so many as those devoted to Mn-diluted magnetic semiconductors (DMS), with Cd_{1-x}Mn_xTe as a typical example. The striking properties observed in these DMS compounds derive from the presence of Mn, which gives rise to *sp*-Mn(3d) and Mn-Mn (*d*-*d*) exchange interactions through the hybridization between the *sp* band and the Mn 3d states.³ Those interactions seem to play a fundamental role also in *H*-MnTe,⁴ not just regarding the magnetic properties but also with relation to the semiconducting properties mentioned above. Another characteristic of Mn-DMS is the evidence of localized Mn $d\rightarrow d^*$ transitions which, apparently, are not present in *H*-MnTe.² One of the key points to understand all these phenomena is the study of its

electronic structure, specially with the aid of optical measurements at different temperatures and pressures. In the following we will review some of the most relevant results on *H*-MnTe, including optical measurements and band-structure calculations, so as to adequately place the aim and outcomes of this work.

Susceptibility⁵ and transport measurements (resistivity,⁵⁻⁷ thermoelectric power^{5,7} and Hall voltage⁷) can be found in the earlier works on *H*-MnTe. MnTe was found to be *p*-type, with a resistivity value around 1 Ω cm and a carrier concentration of 10¹⁸ cm⁻³, both at room temperature. Different Néel temperature values have been reported, such as $T_N=307$ K (or $T_N=310$ K) from the slope change in the resistivity vs temperature curve⁶ (susceptibility vs temperature curve)⁵ and $T_N=328$ K from the maximum in the susceptibility curve.⁵ The latter value is also consistent with that reported by Banewicz *et al.*⁸ ($T_N=323$ K). The discrepancy between the different values is apparent since, as pointed out by Uchida *et al.*,⁵ they stem from the different criteria (maximum or slope change) followed in each case. Both temperature values have been recently confirmed from susceptibility measurements on the same MnTe samples studied in this paper.⁹ Resistivity measurements under pressure up to 1 GPa carried out by Ozawa *et al.*⁶ have yielded an interesting result, i.e., a positive pressure coefficient of the Néel temperature, with a value of $dT_N/dP=+26$ °C/GPa. Accordingly, an increment of the exchange interaction, or equivalently, of the Mn magnetic moment, can be expected with pressure.

The measurements carried out by Allen *et al.*² and Zanmarchi¹⁰ are practically the only available information about optical properties of *H*-MnTe. Allen *et al.* measured the reflectivity up to 5 eV, and the transmission in the infrared range. The calculated absorption coefficient spectrum

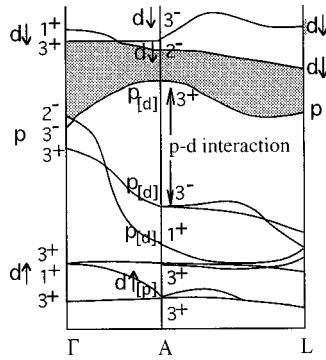


FIG. 1. Schematic band structure of H -MnTe at some points of interest from Ref. 4. At the A point there is a higher degree of hybridization, thus the predominant orbital character is indicated by the first letter, and the secondary by a lower sized letter in brackets.

showed a steep edge at 1.3 eV, which was identified as a direct gap; however, significant absorption below such energy value might suggest the existence of an indirect gap. An example¹¹ from some existing reflectivity spectra by Kendelewicz¹² seems to be in general agreement with Allen's example. Zanmarchi's absorption measurements, also at room temperature and pressure, yielded a band gap of 1.25 eV at 300 K, although any supplementary information can be hardly obtained due to normalization and offset problems. Localized Mn $3d$ atomiclike transitions seem to be absent in the previous absorption spectra but no definitive conclusions can be drawn just from the available data.

A few electronic structure calculations on H -MnTe have been reported. Allen *et al.* gave the first qualitative model, in which the valence bands are Te $5p + \text{Mn } 3d$ spin-up (\uparrow) states (with the $d\uparrow$ states embedded in the p states) and the conduction band as Mn $3d\downarrow + \text{Mn } 4s$ states. The direct optical gap of 1.3 eV determined by Allen *et al.* was introduced as a parameter in two non-self-consistent band-structure calculations, carried out by Sandratskii *et al.*¹³ and Podgórny and Oleszkiewicz,¹¹ respectively. Both calculations gave a similar qualitative picture of this material and confirmed the validity of the Allen *et al.* model. According to them, the valence-band maximum (VBM) is located at the A point in the first Brillouin zone and the conduction-band minimum (CBM) in the vicinity of the L point. In both cases an indirect band gap is obtained at the L point, with an energy of 0.8 eV (Sandratskii), 0.35 eV (Podgórny with warping correction), or 0.8 eV (without warping correction). According to Sandratskii *et al.*, the valence band has a strong hybridized p - d character and the exchange interaction is approximately 4 eV. Instead, Podgórny and Oleszkiewicz give a stronger s - d hybridization in the conduction band, a deeper position for the Mn $3d$ spin-up band into the Te manifold, and a higher Mn energy splitting of 6 eV, due probably to the introduction of a higher Mn magnetic moment ($5\mu_B$ instead of $4.7\mu_B$ adopted by Sandratskii).

The first *ab initio* self-consistent total-energy and band-structure calculation has been carried out by Wei and Zunger.⁴ As it is depicted in Fig. 1, in accordance with the previous calculations, an indirect band gap of -0.19 eV is found, being the VBM located at the A point and the CBM at the L point. Instead, a direct band gap of 0.21 eV is found at the A point. The energy separation between the occupied Mn

$3d$ states, located under the p states, and the unoccupied Mn $3d$ states at the bottom of the conduction band, is 4 eV. Both the Mn bands splitting as well as the band-gap values have been obtained by introducing a magnetic moment of $4.07\mu_B$ in the calculation, but are slightly increased when a higher Mn magnetic moment is adopted (indirect and direct gap energies of 0.3 and 0.71 eV, respectively, for $\mu = 5.5\mu_B$). At the A point, the p states with 3^+ symmetry (3^- symmetry) are raised (lowered) by the conduction-band empty Mn 3^- states and the valence-band occupied Mn 3^+ states (see Fig. 1). This explains why the VBM occurs at A point and why the direct band gap of H -MnTe is smaller than that of MnTe in zinc-blende structure.

The energy splitting of the Mn states found in the previous calculation is relatively small (4 eV), if compared to an energy of 6.6 eV obtained by Sato *et al.*¹⁴ from density of states (DOS) measurements by means of inverse photoemission spectroscopy (IPES), and photoemission spectroscopy (PES), spectroscopy. A linear extrapolation of the leading edge in these measurements yielded a separation of 0.9 eV between the VBM and the CBM. Both experimental results indicate that, as expected from a local-density approximation, the energy scale has probably been underestimated in the band-structure calculation.

To summarize, even if the different calculations of the electronic structure are in agreement in general terms, they arrive to different descriptions of the position of the Mn bands and the magnitude of their splitting or to different character assignments to the electronic states and their degree of hybridization. On the other hand, the optical measurements on H -MnTe have been scarce, both qualitatively and quantitatively, consequently a comprehension of the electronic structure has not been attained from the experimental point of view.

The aim of this work is to provide additional information in this sense. This paper reports on light transmission measurements at different temperatures and pressures in the vicinity of the fundamental absorption edge. The temperature and pressure coefficients of H -MnTe will be calculated, and the temperature and pressure dependence of the absorption spectra will be discussed in terms of the band-structure calculations and the second-order contributions, leading to a better understanding of the role of the d - d and p - d interactions in H -MnTe.

II. EXPERIMENTAL SETUP

In this study we use unoriented samples from a MnTe ingot grown by the traveling heater method (THM).¹⁵ In order to avoid or reduce contamination effects, a low-temperature synthesis process was used. Details on the crystal-growth procedure have been reported elsewhere.⁹

Optical-absorption measurements at ambient pressure and temperatures in the range 16–300 K were carried out in a He closed-cycle cryogenic system. In this case the MnTe samples were cut with a wire saw, mechanically polished with diamond powder, and etched with a 3% solution of bromine in methanol. The sample surface was approximately $5 \times 5 \text{ mm}^2$ and the thickness ranged between 0.1 and 1 mm. Optical-absorption measurements under pressure up to 10 GPa were performed in a membrane diamond anvil cell^{16,17}

(MDAC) at room temperature. In this case the MnTe samples were unpolished splinters with a surface of $100 \times 100 \mu\text{m}^2$ and a thickness of $20 \mu\text{m}$, so as to fit in the MDAC. They were placed together with ruby chips in a $200\text{-}\mu\text{m}$ -diam hole, drilled in a $60\text{-}\mu\text{m}$ -thick inconel gasket. A 4:1 methanol-ethanol mixture was used as pressure transmitting medium to ensure hydrostatic conditions. The pressure was measured from the shift of the R_1 line of the ruby fluorescence with respect to a neon lamp line ($\lambda = 703 \text{ nm}$).

The optical source was a tungsten lamp chopped at 180 Hz. The light from the lamp was collimated and focused on the cryogenerator sample holder or the MDAC and the transmitted light was again collimated and focused on the entrance slit of a THR 1000 Jovin-Ivon monochromator. The detector was a Si photodiode in the case of measurements at variable temperature whereas for measurements under pressure a Ge and a $\text{In}_x\text{Ga}_{1-x}\text{As}$ photodiodes were also used in order to follow the redshift of the absorption edge. The detector signal was synchronously measured with a lock-in amplifier with an output to the acquisition system. The transmittance was measured using the sample-in sample-out method, which, in measurements under pressure, consisted of measuring the intensity transmitted by the sample and normalizing it to the intensity transmitted by a clear area near to it. Stray light was measured in the high absorption region of the sample, and the minimum transmitted intensity was subtracted from every spectrum. Then a correction was made to the experimental transmittance by adjusting it to the theoretical value in the region where the sample is transparent to light. Finally, the absorption coefficient (α) was calculated taking into account the corrected transmittance, the thickness and the reflectivity of the sample.

The MnTe refractive index was determined from the interference pattern at photon energies below the absorption edge (1.6–1.7 eV). For that purpose the sample thickness was measured with a micrometer.

III. EXPERIMENTAL RESULTS AND DISCUSSION

The MnTe refractive index measured with the fringe method in the range $1.6\text{--}1.7 \mu\text{m}$ has a value of $n = 2.46 \pm 0.02$. This value is lower than that reported by Zanmarchi¹⁰ ($n_{\perp} = 3.24 \pm 0.01$) or the one which can be deduced from Allen *et al.*'s reflectivity measurements² ($n_{\perp} = 3.42$, practically constant in the $1\text{--}10\text{-}\mu\text{m}$ interval). And it appears also low in comparison with the values reported² for MnSe ($n = 2.82$) or MnS ($n = 2.6$). Our result, being obtained on nonoriented samples is, however, not directly comparable with the literature values of n_{\perp} , owing to the possible existence of an anisotropy in the refractive index.

The inset (a) in Fig. 2 depicts the MnTe absorption spectrum, measured at 1 bar and 295 K for polished samples of different thicknesses (1 mm, $300 \mu\text{m}$, and $155 \mu\text{m}$) and also with an unpolished thin sample ($20 \mu\text{m}$) inside the MDAC. The spectra are coincident, with the exception of that obtained with the thinnest sample in the MDAC. A high degree of scattered light affected the transmission measurement on such unpolished splinter sample, leading to an apparent absorption rise at the lower energies. If the diffusive part of the spectrum, which follows a straight line, is subtracted, the resultant absorption spectrum agrees with the other spectra

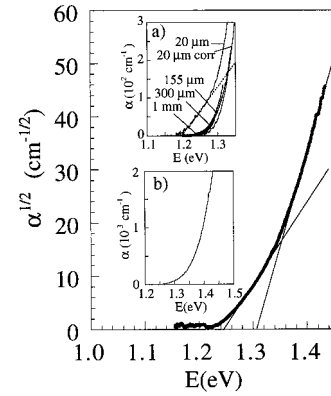


FIG. 2. Inset (a) shows the absorption spectra obtained for samples of different thicknesses (1 mm, $300 \mu\text{m}$, $155 \mu\text{m}$, and $20 \mu\text{m}$). The $20\text{-}\mu\text{m}$ sample spectrum is shown before and after the subtraction of the linear part at low absorption values to eliminate the effect of scattered light (dashed line). Inset (b) shows the MnTe absorption spectrum from the composition of the previous spectra. Main figure: two linear fits can be carried out if the square root of the absorption spectrum is represented, indicating the indirect character of the electronic transitions.

within their absorption range. This agreement has allowed the composition of an absorption spectrum [inset (b)] in Fig. 2, in which the lower absorption values are those obtained from the thicker samples data (1 mm and $155 \mu\text{m}$) and the higher absorption ones, from the thinnest sample ($20 \mu\text{m}$) data. The square root of such composed absorption spectrum, illustrated in the main figure, can be fitted with two straight lines with different slopes, indicating that the measured absorption spectrum is indirect [indirect band gap (ig)]. The crossings of such linear fits with the energy axis give the phonon-absorption energy $E_{\text{ig-ph}} = E_{\text{ig}} - E_{\text{ph}}$ (which is derived from the $155\text{-}\mu\text{m}$ sample data mainly) and the phonon-emission energy $E_{\text{ig+ph}} = E_{\text{ig}} + E_{\text{ph}}$ (determined basically by the $20\text{-}\mu\text{m}$ sample data). An indirect band-gap energy $E_{\text{ig}} = 1.272 \pm 0.013 \text{ eV}$, and a phonon energy of 34 meV is obtained from the average of the previous energies.

This value is consistent with those reported by Zanmarchi¹⁰ (1.25 eV) and Allen *et al.*² (1.3 eV). It must, however, be observed that these authors attributed a direct character to their absorption spectra. As described in the Introduction, Allen *et al.*'s result² was introduced as a constraint in two MnTe band-structure calculations^{11,13} which yielded indirect band gaps of 0.8 and 0.35 eV, respectively. *Ab initio* calculations by Wei and Zunger⁴ resulted in an indirect and direct band gaps of -0.19 and 0.21 eV , respectively, for a magnetic moment of $4.07 \mu_B$. As mentioned previously, both values, together with the exchange, increase when a higher Mn magnetic moment is adopted in the calculation (0.3 and 0.71 eV , respectively, for $\mu = 5.5 \mu_B$). Sato *et al.*'s measurements¹⁴ yielded an exchange splitting of 6.6 eV which is larger than the calculated one, consistently with a larger indirect band gap of 0.9 eV , which is closer to our gap energy determination. To summarize, according to the different band-structure calculations *H*-MnTe is expected to present an indirect band gap, and a direct transition at a slightly higher energy. Our measurement yields a band gap of 1.27 eV whose indirect character is in agreement with the band-structure calculations. Consequently, a direct absorp-

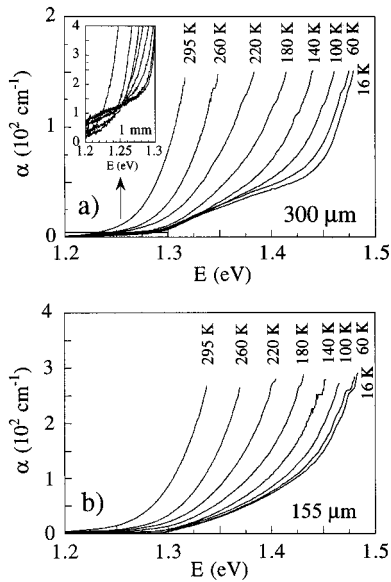


FIG. 3. Absorption spectra at different temperatures for a sample thickness of (a) $d=300\ \mu\text{m}$ (in the inset $d=1\ \text{mm}$ in detail) and (b) $155\ \mu\text{m}$.

tion edge should appear over and around 1.4 eV, our maximum measured energy. The band-gap absolute values cannot be used for comparison due to the fact that a direct band gap of 1.3 eV was introduced as a constraint in two band-structure calculations, and the energies were underestimated in the calculation by Wei and Zunger. Localized Mn-Mn 3*d* transitions are absent in our spectra, consistently with the predicted (4 eV) and measured (6.6 eV) energy between the Mn bands.

Figure 3(a) depicts MnTe absorption spectra at different temperatures ranging from 300 to 16 K for a 300- μm sample. The absorption edge shifts towards higher energies for decreasing temperatures but at about 180 K an anomalous absorption feature appears and becomes more evident as the temperature is progressively lowered. Such absorption onset, which starts at about 1.3 eV, shows a negligible shift with temperature. The inset figure shows the spectrum obtained with a thicker sample (1 mm), so as to evidence the low absorption region in which two smoothly increasing absorption features are also appearing at 220 and 140 K.

As in Fig. 3(a), Fig. 3(b) shows the absorption spectra at different temperatures for the 155- μm sample. A similar behavior is observed, even if the anomalous absorption shape is different and contributes in a larger proportion (up to 80–100 cm^{-1}) to the total absorption. This onset is not attributable to Mn (*d-d*) transitions, in view of the energy separation between occupied and unoccupied Mn 3*d* states.

A first hypothesis which seemed plausible was the presence of an oxide layer on the sample surface. MnTe is known to be highly reactive and hence to oxidize very easily in air. Consequently, a thin layer of MnO or TeO might have appeared on the samples surface, introducing an extra absorption. In order to verify such a hypothesis, we have carried out absorption measurements at 16 K on a sample which was chemically etched so as to eliminate any oxide layer, and then heated in air at temperatures in the range 100–300 °C during different time intervals, in order to accelerate a possible oxidation process. A change of color (from metallic to

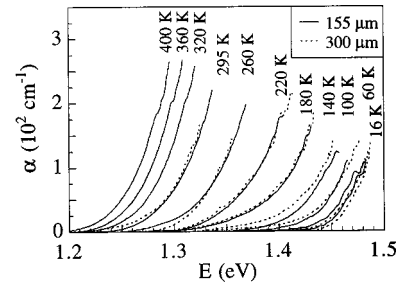


FIG. 4. Absorption spectra at different temperatures after the correction for the anomalous nonshifting absorption feature for the 155- μm sample (solid lines) and the 300- μm sample (dashed lines).

blue) was observed on the sample surface, indicating the formation of a transparent oxide layer of an approximate thickness of 0.1 μm . The intensity transmitted by the sample decreased slightly after the successive sample heating cycles, and an absorption tail progressively appeared at energies below the fundamental edge. But no changes were observed in the anomalous absorption spectrum which was present even in the clean sample and did not increase with the oxidation of the surface. Nevertheless, even if the anomalous absorption had been the contribution of a surface oxide, there would have not been any reason to expect a negligible shift.

Another possible explanation might lie in the presence of impurity levels in the band gap, moving with temperature at the same rate one of the bands does. It is known that the absorption spectrum from a band to an impurity deep level follows a square-root law for allowed transitions and a 3/2 exponent law for forbidden transitions.¹⁸ The anomalous absorption part of the spectrum in Fig. 3(a) can be fitted by a combination of two or more forbidden transitions, as well as by the sum of forbidden and allowed transitions. In the case of Fig. 3(b), the anomalous absorption part follows a 3/2 exponent law. The same could be said about the low absorption tails that appear in the 1-mm sample spectrum. As stated in the Introduction, MnTe is known to be *p* type, due probably to an excess of tellurium content which leads to manganese vacancies that act as acceptors. The resistivity of our samples⁹ is of the same order of magnitude (1 $\Omega\ \text{cm}$) which can be found in the literature^{5,10,15} in *p*-type samples. In those cases, an impurity concentration of about $10^{18}\ \text{cm}^{-3}$ was measured.¹⁰ As the native acceptors are expected to be Mn vacancies, whose ground and excited states are related to Te dangling bonds, it seems reasonable to assign the anomalous absorption to transitions between the valence band and excited states of the Mn vacancy. As both the initial and final states are related to p_z Te states, a negligible shift with temperature can be expected.

The presence of the anomalous absorption feature, whose origin we have just discussed, hinders the calculation of the gap energy shift with temperature. Thus, we have fitted such part at 16 K, and we have subtracted it to the absorption spectrum at all the temperatures, for both the 155- and 300- μm samples. Figure 4 depicts the resultant absorption spectra for the 155- μm sample (solid lines), which are practically coincident with the 300- μm sample spectra (dashed lines) at the different temperatures. Such a coincidence is particularly relevant, as different fitting functions were considered in each case. We have also included in this figure the

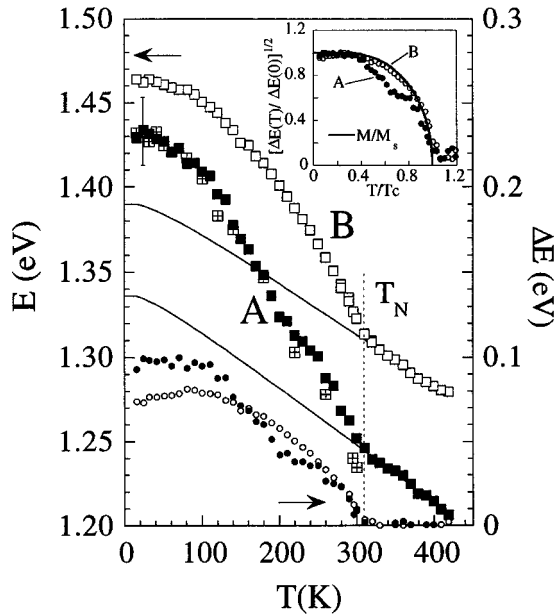


FIG. 5. A: Temperature dependence of the gap energy (phonon-absorption contribution) for the 155- μm sample (black squares) and the 300- μm sample (crossed squares) after the correction for the anomalous part. B: (white squares). Temperature dependence of the energy for an absorption coefficient $\alpha=200\text{ cm}^{-1}$. The solid lines represent a Varshni function fit ($\theta=60\text{ K}$) of the linear part for $T > T_N$. The difference between the experimental data A (or B) and the Varshni-like function is represented by black (white) circles (right-hand y axis). The inset figure represents the normalized square root of those points together with the normalized sublattice magnetization (solid line).

absorption spectra measured at temperatures up to 420 K. In all cases the square root of the absorption coefficient has been plotted and fitted with a straight line whose intercept with the energy axis represents the phonon-absorption contribution to the indirect transition, $E_{\text{ig-ph}}$ (note that the low-energy part of the absorption coefficient at 300 K comes from transmission measurements carried out with the thickest samples).

Data A in Fig. 5 show the temperature dependence of this indirect transition energy $E_{\text{ig-ph}}$ for the 155 μm (black squares) together with some values obtained with the 300- μm sample (crossed squares) which, as we pointed out, are consistent with the previous ones. The error bar on the left indicates the maximum uncertainty in the slope calculation from the linear least-squares fit. Data B represent the photon energy for an absorption coefficient $\alpha=200\text{ cm}^{-1}$ from noncorrected absorption spectra (white squares), and follows a similar temperature dependence.

The temperature variations of the semiconductor band gaps are usually well described by a Varshni equation of the type $E_g(T) = E_g(0) - aT^2/(T + \theta)$, with a zero derivative for $T \rightarrow 0\text{ K}$, and a constant value at high temperatures. A departure from the Varshni-like behavior is evident in this case, in which a slope change is clearly observed in both curves at 310 K, which is the Néel temperature.

An effect of the antiferromagnetic transition on the optical edge has been reported in other antiferromagnetic compounds¹⁹ and in particular in chalcogenides²⁰ such as CoO, $\alpha\text{-MnS}$ (in which an extra blueshift was found below

the Néel temperature) and MnO (in which a redshift was observed). An extra shift to higher energies has been also reported in $\text{Cd}_{1-x}\text{Mn}_x\text{Te}$ and other DMS below the Néel temperature³ and attributed to a change in the magnetic ordering.

The temperature dependence of the resistivity and of the absorption edge of different magnetic systems, and specifically of antiferromagnetic semiconductors, has been predicted by Alexander *et al.*²¹ from calculations that deal with the effect of the critical spin fluctuations on the conduction band. Their predicted temperature dependence agrees with the observed blueshift in the mentioned antiferromagnetic semiconductors. In the specific case of the antiferromagnetic chalcogenides the magnetic transition was found to be accompanied by a crystallographic transition and the absorption edge was attributed to electronic transitions from the magnetic ions to the conduction band. A model²² that included the lattice distortion effect as well as the magnetic ordering effect in the magnetic ions and carriers (the model of Rys *et al.*)²² was able to explain the shift observed in those cases. Ando *et al.*²³ have carried out a second-order perturbation calculation which includes the exchange interaction of electrons in the conduction band and different types of holes in the valence band with fixed Mn spins. According to their results, when the conduction-band shift is dominant, a blueshift proportional to the square of the sublattice magnetization (and consequently having the same temperature dependence) is obtained. Instead, when the valence-band contribution is dominant, the situation is more complex as the second-order energy includes two terms, a positive and a negative one, which may lead to a redshift (negative result) or blueshift (positive result), depending on their relative values. In the particular case in which the ordering effect is small (this should be the case of $\text{Cd}_{1-x}\text{Mn}_x\text{Te}$ and ZB-MnTe) a blueshift which is also proportional to the square of the magnetization is obtained.

In our case, the temperature dependence of the energy gap (data A) is qualitatively in agreement with that of the previously mentioned AF compounds and with the temperature behavior predicted by Alexander *et al.*²¹ At temperatures over the Néel temperature it follows a straight line which corresponds to the linear part of a Varshni-like temperature dependence, and the same can be said about data B. At the Néel temperature a slope change, attributable to a change in the magnetic ordering, appears. We have fitted the points at $T > T_N$ with a Varshni function $E(T)$ (solid lines in Fig. 5), by assuming a typical value for $\theta=60\text{ K}$ (for CdTe $\theta=65.4\text{ K}$, for example). The difference between the experimental points at $T < T_N$ and the fitted curve $E(T)$ represents the magnetic blueshift $\Delta E(T) = E_{\text{exp}}(T) - E(T)$, where E_{exp} are either A or B data (black or white circles, respectively). At 0 K the energy shift reaches its maximum value $\Delta E(0) \approx 0.1\text{ eV}$, which is of the same order of magnitude obtained for ZB-MnTe.²⁵ The dependence of the square root of the blueshift normalized to its maximum value, i.e., $[\Delta E(T)/\Delta E(0)]^{1/2}$, on the relative temperature T/T_N is shown in the inset figure on the upper right for curves A and B in Fig. 5. The theoretical relative magnetization (M/M_s) of a ferromagnetic material, from the well-known expression $M/M_s = \tanh(MT_N/M_s T)$ has been also plotted. The coincidence between the experimental and theoretical curves indi-

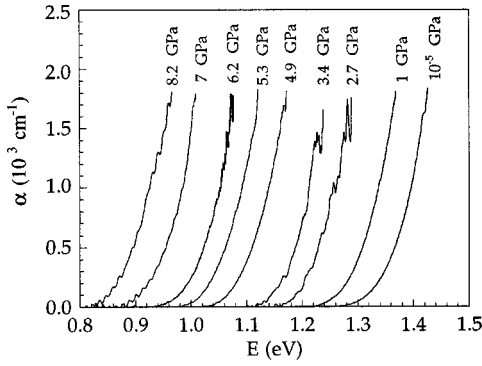


FIG. 6. Absorption spectra at different pressures ($d=20\ \mu\text{m}$).

icates that the energy blueshift found in $H\text{-MnTe}$ is attributable to a change in the magnetic ordering as explained in the previous paragraph. The magnetic shift in data *A* deviates from the theoretical temperature dependence in the range 140–200 K, due probably to an underestimation of $E_{\text{ig-ph}}$ derived from the subtraction of the anomalous absorption fitting curve in an energy range in which it is overestimated. The fact that the shift is positive leaves an uncertainty on which contribution is dominant as, according to the model of Ando *et al.*,²³ either the conduction band or the valence band (if the ordering effect is small) might be contributing.

To summarize, the temperature dependence of the gap energy $E_{g\text{-ph}}$ is a result of two contributions: a classical Varshni function and a term proportional to the square of the magnetization, as follows:

$$E_{g\text{-ph}} = E_0 + \frac{\alpha T^2}{T + \theta} + \Delta E(0) \left(\frac{M}{M_s} \right)^2 H(T_N - T), \quad (1)$$

where

$$E_0 = 1.336 \pm 0.004\ \text{eV},$$

$$\alpha = -(3.5 \pm 0.1) \times 10^{-4}\ \text{eV/K},$$

$$\Delta E(0) = 0.098 \pm 0.001\ \text{eV},$$

and $H(T_N - T)$ is the Heaviside unit step function. Note that θ was arbitrarily chosen equal to 60 K, thus, errors are just indicative of the uncertainty at a fixed θ value. Very similar results are obtained if θ is varied within ± 10 K.

Absorption spectra at different pressures carried out with the sample in the MDAC are shown in Fig. 6, for a 20- μm sample. Diffraction studies of $H\text{-MnTe}$ up to 6.7 GPa (Ref. 24) have not revealed any phase transition which, according to our measurements, does not take place even at 12.2 GPa. We were not able to measure the absorption spectrum at that pressure as it involved photon energies that were below the detector threshold. However, the spectrum at a lower pressure such as 5 GPa was the same before and after applying 12 GPa to the sample. The occurrence of a phase transition is very unlikely, as it would normally result in a polycrystalline sample and an increased light scattering that was not observed.

As explained in the experimental setup section, in this set of measurements the samples introduced in the MDAC were unpolished splinters, with the consequence that a high level of scattered light was present in the transmitted intensity. It

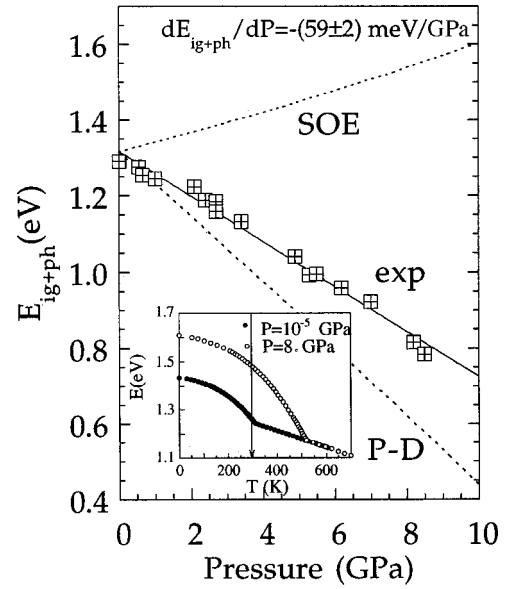


FIG. 7. Pressure dependence of the gap energy (phonon-emission contribution): experimental points (crossed squares) and linear fit (solid line). The observed dependence has been attributed to two competing mechanisms: a blueshifting one derived from the increase of the exchange interaction with pressure (curve SOE) and a redshifting one from an enhancement of the p - d repulsion (curve P - D).

has been corrected by the same fitting procedure explained in a previous paragraph at the beginning of this section, allowing, at least, for a proper determination of the phonon-emission part of the indirect absorption curve, $E_{\text{ig-ph}}$. Instead, the phonon-absorption contribution cannot be obtained as it is affected by a large error. Figure 7 depicts the pressure dependence of $E_{\text{ig-ph}}$. A slightly sublinear dependence is observed, but deviations from linearity are small enough in this range to justify a linear fit which yields the pressure coefficient

$$\frac{dE_{\text{ig-ph}}}{dP} = -(59 \pm 2)\ \text{meV/GPa}. \quad (2)$$

Typical pressure coefficients are, for example, the positive values 80 meV/GPa in CdTe ,²⁵ 46 meV/GPa in $\text{Cd}_{0.3}\text{Mn}_{0.7}\text{Te}$,²⁶ or 63.4 meV/GPa in $\text{Zn}_{0.75}\text{Mn}_{0.25}\text{Te}$ (Ref. 27) among others, whereas a negative pressure shift is obtained in this case.

There is some information related to this point which is worth taking into account. As reviewed in the Introduction, a previous study on the effect of pressure on the Néel temperature of NiAs-MnTe by Ozawa *et al.*⁶ reported a linear pressure dependence, with a coefficient of $dT_N/dP = 26\ \text{K/GPa}$. This positive pressure shift can be attributed to an increment of the exchange interaction or, equivalently, to an increment of the sublattice magnetization with pressure which can produce two effects: first, a shift of the curve representing the temperature dependence of the gap energy (such as data *A* in Fig. 5) towards higher temperatures with increasing pressure; second, an increment of the second-order magnetic blueshift, as it is proportional to the square of the sublattice magnetization. On the assumption that the Néel temperature is proportional to the exchange interaction, and on the basis of the known experimental maximum blueshift at ambient pressure

$\Delta E_{\max}(0)=0.098$ eV, it is possible to calculate $\Delta E(P) = \Delta E(0) [T_N(P)/T_N(0)]^2$. When pressure is applied to MnTe at a fixed temperature (295 K) up to 8 GPa, for example, the Néel temperature moves from 310 to 518 K and the energy vs temperature curve with it. Additionally, the magnitude of the energy shift increases. The result is depicted in the inset in Fig. 7, where points calculated from Eq. (1) have been plotted for $P = 10^{-5}$ GPa and $P = 8$ GPa. Thus, an increment of 0.22 eV in the gap energy should be observed at 295 K (an average pressure coefficient of 28 meV/GPa approximately). On the contrary, we observe the gap energy to redshift with pressure, which means that the mechanism which leads to the negative shift is actually larger than the one which produces the positive shift. Let us interpret these phenomena in the framework of the MnTe band structure. A positive pressure shift of the Néel temperature indicates an increase of the exchange interaction due to the reduction of the interatomic spacings with pressure, and hence to an increment of the energy separation between the occupied and empty Mn ($3d$) levels. According to the band-structure calculation by Wei and Zunger,⁴ the introduction of a higher Mn magnetic moment increases not only the exchange splitting but also the band-gap separation. Consequently, a first-order positive-energy shift should be added to the previous second-order energy blueshift, dependent on the square of the magnetization. Thus, the expected blueshift should be even larger. However, we have not been able to estimate that first-order contribution, as no experimental values of the Mn splitting as a function of pressure are available. The second-order blueshift value at 295 K has been calculated at all pressures from Eq. (1) and is plotted in Fig. 7, with the label SOE (second-order energy).

On the other hand, according to the band structure the indirect absorption edge is related to transitions between the VBM located at the A point and with a p character, and the CBM, located at the L point and with a d character. As explained in the Introduction, according to the model by Wei and Zunger, the low-energy gap in H -MnTe, together with the fact that the valence-band maximum is located at the A point, has been attributed to a p - d repulsion which raises p states with 3^+ symmetry and lowers the p states with 3^- symmetry (Fig. 1). A possible explanation for the experimental negative pressure shift might lie in an enhancement of such p - d repulsion with pressure, which would shift upwards the valence-band maximum. Curve P - D in Fig. 7, obtained from the difference between the experimental and the curve SOE, represents the energy redshift attributed to such mechanism. To summarize, the increment of the exchange interaction with pressure would increase the second-order energy at the rate indicated by curve SOE (28 meV/GPa average), but the enhancement of the p - d repulsion would raise the top of the valence band at an average rate of 87 meV/GPa (curve P - D), yielding an overall experimental band-gap shift of -59 meV/GPa. A theoretical calculation of

the bands contribution to the second-order perturbation energy should indicate which band is dominant in the band-gap blueshift below the Néel temperature. We must recall that the first-order energy shift (the band gap increases with pressure) has not been included, hence the previous theoretical pressure coefficients are underestimations of the real shifts.

IV. SUMMARY

The temperature and pressure dependence of the optical absorption of hexagonal (H) (NiAs structure) antiferromagnetic (AF) MnTe has been determined by means of transmission measurements at ambient pressure in the range 16–300 K and at ambient temperature and pressures up to 9 GPa ($T=295$ K). The square root of the absorption spectrum shows a linear dependence with two different slopes, from which an indirect gap of energy $E_{ig}=1.272\pm 0.013$ eV has been obtained. Such indirect character is in agreement with different band-structure calculations and, to the best of our knowledge, it constitutes its first experimental confirmation. The temperature dependence of the absorption edge is linear above the Néel temperature $T_N=310$ K, with a temperature coefficient $dE/dT=(3.5\pm 0.1)\times 10^{-4}$ eV/K. Below T_N an extra blueshift is found, with a maximum value of 0.1 eV at low temperatures. Such blueshift has been reported in different magnetic and semimagnetic compounds and it has been attributed to the interaction between electrons in the conduction band (or holes in the valence band) and the magnetic ions that are present, interaction which depends on the magnetic ordering. In this case, the temperature dependence of such an anomalous shift is found to be proportional to the square of the magnetization, a result which is consistent with the second-order perturbation calculations carried out by Ando *et al.*²³ The pressure dependence of the gap energy follows almost a straight line with a negative pressure coefficient $dE/dP=-(59\pm 2)$ meV/GPa. The Néel temperature is known to increase with pressure in AF- H -MnTe due to an increment of the exchange interaction, or equivalently, of the sublattice magnetization. Such increment is expected to cause a shift towards higher temperatures of the gap energy-vs-temperature curves and also to increase the extra blueshift attributed to the magnetic ordering. Both effects should lead to a blueshift of the second-order energy with pressure when measured at a fixed temperature. The negative coefficient has thus been interpreted as the sum of two contributions, the previous positive one, related to the increased exchange interaction, and a larger negative one derived from an enhancement of the p - d repulsion at the A point, leading to an upwards shift of the valence-band maximum with pressure. Our results are thus consistent with the H -MnTe electronic structure calculations obtained by Wei and Zunger.⁴

ACKNOWLEDGMENTS

This work was supported by the Spanish government CICYT Project Nos. MAT95-0391 and MAT98-0975-C02-01.

*Electronic address: Chantal.Ferrer@uv.es

¹S. M. Durbin, J. Han, O. Sungki, M. Kobayashi, D. R. Menke, R. L. Gunshor, Q. Fu, N. Pelekanos, A. V. Nurmikko, D. Li, J. Gonsalves, and N. Otsuka, Appl. Phys. Lett. **55**, 2087 (1989).

²J. W. Allen, G. Lukowsky, and J. C. Mikkelsen, Jr., Solid State Commun. **24**, 367 (1977).

³*Diluted Magnetic Semiconductors*, edited by J. K. Furdyna and J. Kossut, Semiconductors and Semimetals Vol. 25 (Academic,

- San Diego, 1988).
- ⁴S. H. Wei and A. Zunger, *Phys. Rev. B* **35**, 2340 (1987).
- ⁵E. Uchida, H. Kondoh, and N. Fukuoka, *J. Phys. Soc. Jpn.* **11**, 27 (1956).
- ⁶K. Ozawa, S. Anzai, and Y. Hamaguchi, *Phys. Lett.* **20**, 132 (1966).
- ⁷J. D. Wasscher and C. Haas, *Phys. Lett.* **8**, 302 (1964).
- ⁸J. J. Banewicz, R. F. Heidelberg, and A. H. Luxem, *J. Phys. Chem.* **65**, 615 (1961).
- ⁹C. Reig, V. Munoz, C. Gómez, Ch. Ferrer-Roca, and A. Segura (unpublished).
- ¹⁰G. Zanmarchi, *J. Phys. Chem. Solids* **28**, 2123 (1967).
- ¹¹M. Podgórny and J. Oleszkiewicz, *J. Phys. C* **16**, 2547 (1983).
- ¹²T. Kendelewicz, Ph.D. thesis, Warsaw University, 1979.
- ¹³L. M. Sandratskii, R. F. Egorov, and A. A. Berdyshev, *Phys. Status Solidi B* **104**, 103 (1981).
- ¹⁴H. Sato, T. Mihara, A. Furuta, M. Tamura, K. Mimura, N. Happo, M. Taniguchi, and Y. Ueda, *Phys. Rev. B* **56**, 7222 (1997).
- ¹⁵R. Triboulet, T. Nguyen, and Duy A. Duran, *J. Vac. Sci. Technol. A* **3**, 95 (1985).
- ¹⁶R. Letoullec, J. P. Pinceaux, and P. Loubeyre, *High Press. Res.* **1**, 77 (1988).
- ¹⁷J. C. Chervin, B. Canny, J. M. Besson, and Ph. Pruzan, *Rev. Sci. Instrum.* **66**, 2595 (1995).
- ¹⁸R. Masut and C. M. Penchina, *Phys. Status Solidi B* **130**, 737 (1985).
- ¹⁹K. W. Blazey and H. Rohrer, *Phys. Rev.* **185**, 712 (1969); G. Bussh and P. Wachter, *Phys. Kondens. Mater.* **5**, 232 (1966); *Solid State Commun.* **8**, 1133 (1970).
- ²⁰H.-h. Chou and H. Y. Fan, *Phys. Rev. B* **10**, 901 (1974).
- ²¹S. Alexander, J. S. Helman, and I. Balberg, *Phys. Rev. B* **13**, 304 (1976).
- ²²F. Rys, J. S. Helman, and W. Baltensperger, *Phys. Kondens. Mater.* **6**, 105 (1967).
- ²³K. Ando, K. Takahashi, T. Okuda, and M. Umehara, *Phys. Rev. B* **46**, 12 289 (1992).
- ²⁴W. Paszkowicz and E. Dynowska, *Acta Phys. Pol. A* **91**, 939 (1997).
- ²⁵G. A. Babonas, R. A. Bendoryus, and A. Yu. Shileika, *Fiz. Tverd. Tela (Leningrad)* **5**, 449 (1971) [*Sov. Phys. Solid State* **5**, 392 (1971)].
- ²⁶G. Ambrazevicius, G. Babonas, S. Marcinkevicius, V. D. Prochukhan, and Yu V. Rud, *Solid State Commun.* **49**, 651 (1984).
- ²⁷S. Ves, K. Strösner, W. Gebhartr, and M. Cardona, *Solid State Commun.* **57**, 335 (1986).